Наносистеми, наноматеріали, нанотехнології
Nanosistemi, Nanomateriali, Nanotehnologii
2021, т. 19, № 4, сс. 799–806

PACS numbers: 61.05.cp, 61.43.Gt, 62.20.Qp, 68.37.Hk, 81.07.Wx, 81.20.Ev, 81.65.Ps

Effect of Production Methods on the Microstructure, Phase Composition, and Properties of Hard Alloy VK8 with Submicron Grain

A. V. Minitskyi[1], P. I. Loboda[1], Ie. G. Byba[1], I. Yu. Trosnikova[1], and O. I. Khovavko[2]

[1]*National Technical University of Ukraine 'Igor Sikorsky Kyiv Polytechnic Institute', 37, Prospekt Pobedy, UA-03056 Kyiv, Ukraine*
[2]*Gas Institute, N.A.S. of Ukraine, 39, Dehtiarivska Str., UA-03113 Kyiv, Ukraine*

The effect of manufacturing process on the microstructure, phase composition, and properties of hard alloy VK8 that can be used for the cores of small armour-piercing ammunitions is revealed. According to the results obtained by scanning electron microscopy, x-ray phase analysis, and durometry, the sintering kinetics of the hard alloy VK8 allows forming a fine-grained microstructure with different levels of microstresses, depending on the production technique, which affects the mechanical properties of the material.

Встановлено вплив методів одержання на мікроструктуру, фазовий склад і властивості твердого сплаву ВК8, що може використовуватися в якості матеріялу для бронебійних сердечників стрілецької зброї. Методами растрової електронної мікроскопії, рентґенофазової та дюрометричної аналіз встановлено, що кінетика процесу спікання твердого сплаву ВК8, залежно від методу одержання, уможливлює сформувати дрібнозернисту структуру з різним рівнем мікронапружень, що формує механічні властивості матеріялу.

Key words: hard alloy, tungsten carbide, spark plasma-enhanced sintering, electron beam-assisted sintering, radiation sintering, hardness, microstresses.

Ключові слова: твердий сплав, карбід Вольфраму, іскроплазмове спікання, електронно-променеве спікання, радіяційне спікання, твердість, мікронапруження.

(Received 29 October, 2021; in revised form, 5 November, 2021)

1. INTRODUCTION

The use of materials in the arms industry requires the development of high performance alloys with a given level of properties. The cores of small armour-piercing ammunitions are the parts to which high requirements are set; they should have a high penetrating ability, which is provided by high kinetic energy and intactness of the core after piercing. This problem is possible to solve by using for the core a material with high strength, hardness, and specific weight. The combination of these characteristics can be achieved by using hard tungsten carbide alloys. However, the use of standard hard alloy manufacturing technologies does not provide maximum hardness and strength due to the growth of tungsten carbide grains during sintering [1–3].

Currently, a mixture of WC–Co fine powders with a particle size of about 1 μm is used in order to provide high mechanical performance of the hard alloys. One of the ways to create a fine-grained microstructure consists in the use of nanosize and submicron hard alloy powders [4–6]. However, the production of nanosize powders is accomplished by their difficult stabilization and requires energy-consuming grinding in planetary mills or attritors that results in contamination of the mixture, as well as intense deformation that increases absorbed energy and ultimately leads to particle growth. A partial solution to this problem consists in manufacturing carbide nanoparticles by synthesis in gas phase chemical reactions, or plasma chemical synthesis, which ensures a narrower particle size distribution and reduces excess energy [7]. However, another problem of nanostructure formation in carbide materials is the process of particle consolidation during sintering. The sintering in the presence of a liquid phase leads to fast grain growth caused by intensive mass transfer [8]. The diffusion processes can be retarded in solid-phase sintering; however, this makes impossible to get rid of residual porosity.

Traditional vacuum technologies of free sintering are not effective for producing hard alloy materials with nanostructures or fine structures. One way to inhibit grain growth in hard-alloy mixtures consists in applying pressure during sintering, which allows reducing the consolidation temperature. Such methods include hot static (HP) and hot isostatic pressing (HIP) technologies [9–11]. However, the disadvantage of these methods is the high probability of formation of residual porosity in the material, because the consolidation is performed mainly in the conditions of solid-phase sintering. A promising method of forming non-porous hard alloys with fine microstructure is spark plasma sintering (SPS), which implements

rapid heating with a rate of about 400–500 degrees per minute [11–13]. Heating with high rate, as well as applied pressure, allow to reduce the sintering temperature to 1200–1300°C. Thus, it is necessary to study in more detail the features of consolidation of the WC-based hard alloys under the conditions of rapid sintering techniques, including those with electron beam application.

The goal of the work is to establish the effect of sintering conditions on the microstructure, phase composition, and properties of a hard WC-based alloy with 8% Co (VK8).

2. EXPERIMENTAL TECHNIQUES

As the object of research, a mixture of VK8 consisting of tungsten carbide (92%) and cobalt bond (8%) with an initial average particle size of 5.5–6.0 μm (determined at laser diffraction analyser Malvern Mastersizer 2000, UK) was selected (Fig. 1, *a*). Since the particle size of the hard-alloy mixture should be less than 1 μm, that is necessary to activate sintering, the mixture was ground in a drum ball mill with ethyl alcohol in a ratio of 1:4 for 120 hours. The average particle size after grinding was 0.80–085 μm (see particle size distribution in Fig. 1, *b*).

After grinding, a part of the mixture was mixed with a plasticizer (solution of rubber in gasoline) in order to provide formability. After mixing with the plasticizer, the mixture was dried in a drying cabinet at 80°C for 3 hours to remove moisture. Then, granulation was performed by rubbing the mixture through a sieve to ensure formability. The formation of the mixture was carried out by static pressing in a hydraulic press under a pressure of 50–100 MPa, using the scheme of bilateral pressing, which is necessary for producing parts with a ratio $H/D > 2$. After forming, the samples were dried in a drying cabinet at 80°C for 3 hours to remove residual moisture.

The compacts were sintered in different ways: sintering in a vacuum

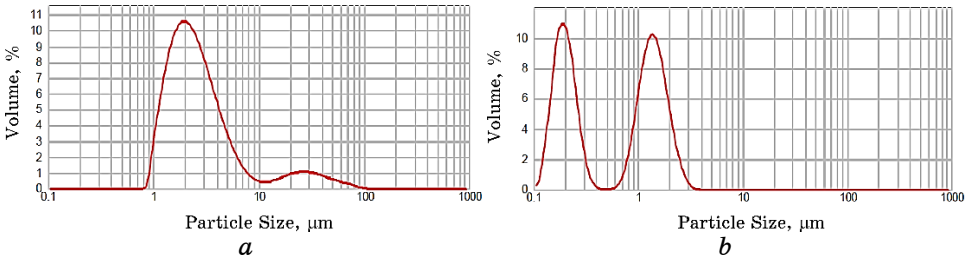

Fig. 1. Particle size distribution of VK8 particles: initial mixture (*a*); after grinding for 120 h (*b*).

furnace, electron beam sintering, and spark plasma sintering. Vacuum furnace sintering was performed in a vacuum electric resistance furnace in graphite backfill (fraction $-1+063$) at 1450 ± 10°C with isothermal annealing for 60 min; the samples were heated with a rate of 200°C/h up to 400°C in order to remove gradually the plasticizer; then, the heating rate was increased to 400°C/h.

Electron beam sintering was performed at ELA-6 unit, which allows implementing sintering of cylindrical samples in both manual and fully automatic mode with rotation around vertical and horizontal axis. The advantage of electron beam heating is the ability to change gradually and in a wide range the quantity of applied heat, as well as the configuration of the heating zone. The unit is equipped with vacuum equipment of Pfeiffer Vacuum GmbH (Germany). Electron beam sintering was performed for 60 seconds in different regimes, depending on the current (4–6 mA).

Spark plasma sintering was carried out in graphite moulds using the unit of KSE®-FCT HP D 25-SD type (Germany) equipped with a 25-ton press and a vacuum chamber (with the possibility of using inert gas). The mixture in a graphite mould was heated with a rate of 300°C/min at a pressure of 25 MPa up to 1380°C and annealed at this temperature for 3 min.

The microstructure of the samples was studied using a scanning electron microscope REM-106I SELMI (Ukraine). X-ray studies of phase composition were performed at a RIGAKU ULTIMA IV diffractometer (Japan) using the Rietveld and Reference Intensity Ratio (RIR) methods with $\mathrm{Cu}K_{\alpha_{1,2}}$ ($\lambda_{\mathrm{Cu}K\alpha 1} = 0.1541$ nm). The microstresses were determined by the Stokes–Wilson method using the software of RIGAKU ULTIMA IV diffractometer [14]. The HRA (Rockwell) hardness was measured at TK-2 unit by indenting the sample surface by a diamond cone according to the standard ISO 4498. The microhardness was measured by the Vickers method on a microhardness tester LHVS-1000Z (China) with a diamond indenter at a load of 1000 g.

3. RESULTS

The studies of the microstructure of the samples produced by different methods showed that the porosity was below 0.5% (Figs. 2, 3) that was confirmed by the results of density measurements by means of hydrostatic weighing; the density of sintered samples was of 14.6 g/cm^3 that corresponds to the theoretical density of the VK8 alloy.

The studies of microstructure also showed that the samples produced by furnace sintering contained small amount of η-phase (Co_3W_3C) inclusions, which was confirmed by the results of local EDS and x-ray phase analyses (Fig. 3).

The hardness of the samples was in the range of 88–94 HRA. The

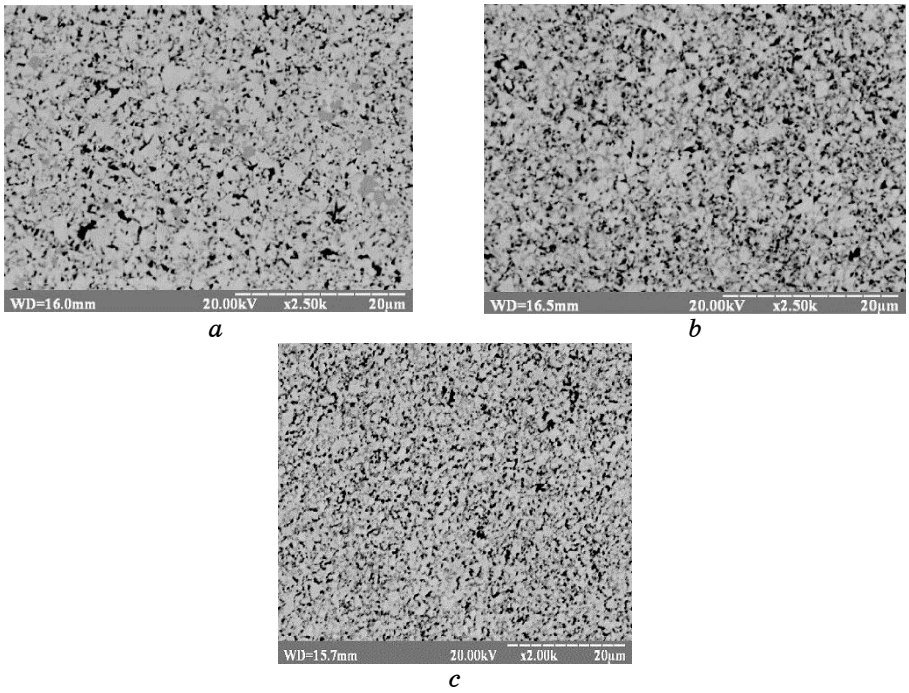

a *b* *c*

Fig. 2. Microstructure of VK8 alloy produced by different methods: vacuum furnace sintering (*a*); electron beam sintering (*b*); spark plasma sintering (*c*).

lowest values corresponded to the samples produced by radiation sintering (88–89 HRA); the samples sintered by electron beam and spark plasma methods had the hardness not less than 93–94 HRA.

The studies of microhardness showed that after furnace sintering the microhardness was about 15.0–15.5 GPa, whereas rapid methods led to its increase up to 17.5–18.0 GPa (Fig. 4).

The microstresses in different phases of the samples produced by different techniques were also determined (Table).

4. DISCUSSION

The results of metallographic studies revealed that the sintering conditions, namely the kinetics of the process, has a significant impact on the formation of the structure of the hard alloy. For example, furnace sintering leads to the formation of a structure with an average grain size of 2–4 μm (Fig. 2, *a*), *i.e.*, grain growth occurs due to recrystallization processes activated by long exposure at high temperatures. Another feature of the microstructure formed upon furnace sintering is the precipitation of a certain amount of the η-

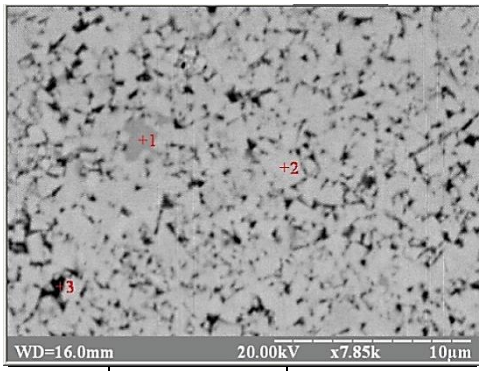

No.	W	Co
1	82.45	16.91
2	99.83	—
3	28.93	65.28

a

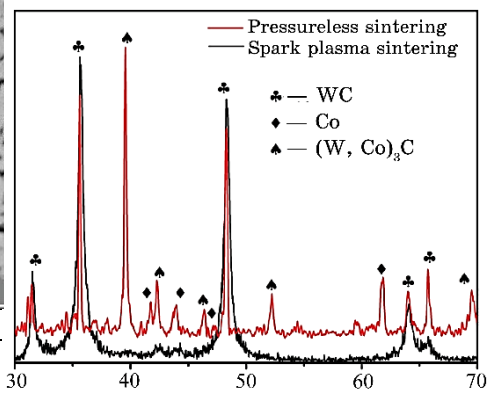

b

Fig. 3. Results of EDS and x-ray phase analyses of VK8 alloy: microstructure and local chemical composition after vacuum furnace sintering (*a*); diffractograms after vacuum furnace and spark plasma sintering (*b*).

phase that is caused by the processes of partial decarburization of the samples. The microstructures of the VK8 alloy after spark plasma and electron beam sintering are somewhat similar to each other (see Figs. 2, *b*, *c*): the grain size is about 1 μm, *i.e.*, almost the same as the size of the particles in the initial powder mixture. It should be also noted that the increase of exposure time during electron beam sintering up to 2 minutes can also lead to the formation of a small amount of the η-phase.

The absence of the η-phase after spark plasma sintering (confirmed by the results of x-ray phase analysis; see Fig. 3, *b*) is explained by the fact that the process was performed in a graphite mould, that prevented decarburization.

The results of durometry confirmed the dependence of the properties on the sintering kinetics: the values of hardness and microhardness fully correlated with the grain size, so the highest hardness and microhardness (93–94 HRA and 17.5–18.0 GPa, respectively) were measured on fine-grained samples after electron beam and spark plasma sintering. At the same time, furnace sintering caused grain growth that resulted in lower hardness and microhardness (88–89 HRA and 15.2–15.5 GPa, respectively).

The level of microstresses is one of the characteristics, which determines the physical and mechanical properties of a material. The measurements of microstresses in the produced samples showed that the highest compressive stresses were observed after spark plasma and

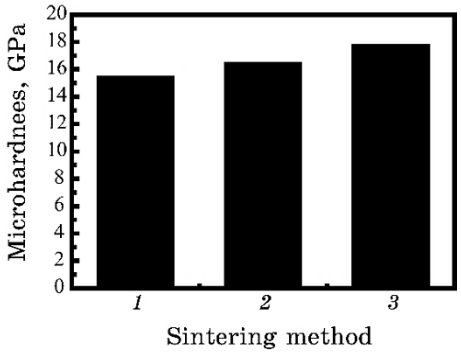

Fig. 4. Microhardness (at load of 1000 g) of VK8 alloy produced by different techniques: vacuum furnace sintering (*1*); electron beam sintering (*2*); spark plasma sintering (*3*).

TABLE. Microstresses in the phase constituents of VK8 alloy produced by different techniques.

No.	Sintering method	Phase composition, %		CSR* size, Å		Microstresses in phases, GPa	
		WC	Co	WC	Co	WC	Co
1	Furnace sintering, exposure time 60 min	94	6	150	235	–4.002	–0.164
2	Electron beam sintering, exposure time 1 min	89	11	365	248	–10.23	–0.69
3	Spark plasma sintering, exposure time 3 min	92	8	101	89	–6.22	–2.66

Note: *Coherent scattering region.

electron beam sintering (see Table). Higher microstresses appeared due to higher sintering rates, which were accompanied by nonequilibrium processes; after electron beam sintering, compressive microstresses in the WC phase reached –10.23 GPa. The lowest microstresses of –4.002 GPa were predictably observed after vacuum furnace sintering with a long isothermal exposure, which is explained by the fullness and completeness of the processes of grain consolidation and partial relaxation of microstresses during slow cooling.

5. CONCLUSIONS

The effect of sintering regimes on the microstructure, phase composition, and properties of the hard alloy VK8 has been studied. It is shown that the conditions of rapid sintering methods, such as spark plasma and electron beam sintering, provide the formation of fine-grained mi-

crostructure, high hardness and microhardness in the hard alloy VK8. The features of the microstructure formation, namely the precipitation of small amount of the η-phase with increasing exposure time during electron beam sintering, are revealed for rapid methods. The correlation between the sintering kinetics and the microstresses in the phase constituents of the hard alloy VK8 is shown.

The studies have shown the prospects of rapid sintering techniques for hard alloys and their advantage over traditional furnace sintering. The results can be used in the development of the cores of small armour-piercing ammunitions.

REFERENCES

1. V. S. Panov and A. M. Chuvilin, *Tekhnologiya i Svoistva Spechennykh Tverdykh Splavov i Izdeliy iz Nikh* (Moscow: Izd-vo MISiS: 2001) (in Russian).
2. R. Kieffer and F. Benezovskij, *Tverdyye Splavy* [Hard Alloys] (Moscow: Metallurgiya: 1971) (Russian translation).
3. P. Schwarzkopf and R. Kieffer, *Cemented Carbides* (New York: Macmillan: 1960).
4. A. F. Lisovskij, *Sverkhtverdyye Materialy*, **6**: 31 (2010) (in Russian).
5. Yu. I. Gordeev, A. K. Abkaryan, A. S. Binchurov, V. B. Yasinskiy, I. V. Karpov, A. A. Lepeshev, O. L. Khasanov, and E. S. Dvilis, *Journal of Siberian Federal University. Engineering & Technologies*, **3**: No. 7: 270 (2014) (in Russian).
6. I. Yu. Trosnikova and P. I. Loboda, *Journal of Superhard Materials*, **41**, No. 1: 49 (2019); https://doi.org/10.3103/S1063457619010076
7. E. A. Levashov, V. S. Panov, and I. Yu. Konyashin, *Izvestiya VUZov. Poroshkovaya Metallurgiya i Funktsional'nyye Pokrytiya*, **3**: 14 (2017) (in Russian).
8. H. Kramar, L. Bodrova, Ya. Kovalchuk, S. Marynenko, and I. Koval, *Scientific Journal of the TNTU*, **3**, No. 91: 25 (2018); https://doi.org/10.33108/visnyk_tntu2018.03.063
9. Xingxing Lyu, Xiaosong Jiang, Hongliang Sun, and Zhenyi Shao, *Nanotechnology Reviews*, **9**: 543 (2020); https://doi.org/10.1515/ntrev-2020-0044.
10. I. Azcona, A. Ordonez, J. M. Sanchez, and F. Castro, *Journal of Materials Science*, **37**, No. 19: 4189 (2002); https://doi.org/10.1023/A:1020048105585
11. Chengchang Jia, Lan Sun, Hua Tang, and Xuanhui Qu, *International Journal of Refractory Metals and Hard Materials*, **25**, No. 1: 53 (2007); https://doi.org/10.1016/j.ijrmhm.2005.11.003
12. E. A. Lantsev, V. N. Chuvil'deev, A. V. Nokhrin, M. S. Boldin, N. V. Malekhonova, Y. V. Blagoveshchenskii, N. V. Isaeva, Y. V. Tsvetkov, P. V. Andreev, and K. E. Smetanina, *IOP Conf. Series: Materials Science and Engineering*, **1014**: 012020; https://doi.org/10.1088/1757-899X/1014/1/012020
13. V. N. Chuvil'deev, A. V. Moskvicheva, M. S. Boldin, N. V. Sakharov et al., *Vestnik Nizhegorodskogo Universiteta im. N. I. Lobachevskogo*, **2**, No. 2: 115 (2013) (in Russian).
14. O. P. Karasevs'ka, I. Yu. Trosnikova, and P. I. Loboda,, *Rentgenostrukturnyy Analiz Materialiv u Dyspersnomu Stani* (Kyiv: Politekhnika: 2017) (in Ukrainian).